

## 5. Experimental studies on rat kidneys

This chapter describes the use of the miniaturized impedance probe in three experimental studies on rat kidneys<sup>1</sup>. The gross objective of these studies was to assess the use of electrical impedance monitoring in kidneys subjected to warm or cold ischemia.

During the MicroCard and MicroTrans projects, other experimental studies about ischemia and impedance on other animals and organs were also carried out. Such studies are presented in part in [2-5].

---

<sup>1</sup> Although impedance measurements on rat kidneys are very rare due to evident practical limitations related to size, it must be noted the early work performed by Lofgren in 1951 [1].

### 5.1. Multiparametric monitoring of ischemia-reperfusion in rat kidney

Ischemic preconditioning, that is, brief ischemic periods before sustained ischemia, has been shown to protect several organs, including the kidney, from ischemia-reperfusion injury. In this study we tested whether the effect of preconditioning could be appraised by real-time measurement of electrical impedance and other parameters that are considered to be representative of tissue hypoxia and that can be measured by employing miniaturized probes.

*Methods.* In a sample of pentobarbital-anesthetized and mechanically ventilated rats, we studied the effect of renal ischemic preconditioning (10-min ischemia and 10-min reflow interval) on subsequent ischemia-reperfusion (45 min and 60 min). Renal tissue electrical impedance magnitude at 1 kHz was measured with the silicon probe described in chapter 2. Extracellular pH and potassium concentration  $[K^+]$  were measured continuously by commercial implanted electrodes.

*Results.* Ischemia induced an early, rapid rise in extracellular potassium and impedance magnitude, followed by a phase of slower increase, whereas pH decreased rapidly, reaching a plateau. Preconditioning treatment did not cause significant changes in interstitial pH and  $[K^+]$  but increased ischemic tissue impedance. During reperfusion, the three variables recovered progressively; however, after a decline, electrical impedance magnitude showed a clear postischemic increase. This rise was suppressed by preconditioning.

*Conclusions.* Real-time measurement of any of the three parameters showed capability for early detection of ischemia. In contrast with findings in myocardial tissue, preconditioning in the kidney did not increase potassium cell loss during ischemia or improve ischemic acidosis or tissue impedance. Electrical impedance magnitude increased for a second time during reperfusion, indicating the presence of a postischemic cellular edema<sup>2</sup>; concealing this episode was the most noticeable effect of the preconditioning treatment.

The following is an extract of :

- Ivorra, A., Gómez, R., Noguera, N., Villa, R., Sola, A., Palacios, L., Hotter, G., and Aguiló, J., "Minimally invasive silicon probe for electrical impedance measurements in small animals," *Biosensors & Bioelectronics*, vol. 19, no. 4, pp. 391-399, 2003.

---

<sup>2</sup> It is interesting to note that quite recently we found out another paper [6] that described an experimental study in which impedance and pH were also simultaneously measured during ischemia-reperfusion. Those experiments were performed on rabbit anterior tibialis muscle but the results shown a phenomenon that was also observed in our case: the pH and the impedance magnitude ( $R_0$ ) are closely related during the development of ischemia but not during reperfusion. In fact, pH tends to recover its basal level but impedance does not reach its original values before the I/R process.

- Sola, A., Palacios, L., López-Martí, J., Ivorra, A., Noguera, N., Gómez, R., Villa, R., Aguiló, J., and Hotter, G., "Multiparametric monitoring of ischemia-reperfusion in rat kidney: effect of ischemic preconditioning," *Transplantation*, vol. 75, no. 6, pp. 744-749, Mar.2003.

### 5.1.1. Introduction and background

Ischemic preconditioning (i.e. brief ischemic periods before protracted ischemia) has been shown to protect against ischemia-reperfusion (I/R) injury in a variety of organs [7]. For monitoring such an injury with miniature sensors, we measured three physical chemical tissue parameters representative of well-documented events occurring during ischemia: extracellular pH, potassium concentration, and electrical impedance. Tissue pH measurement is regularly used to measure tissue hypoxia [8]. The use of surface pH and PCO<sub>2</sub> electrodes has also been proposed to detect ischemia in the kidney [9;10]. In regard to extracellular [K<sup>+</sup>], early increases have been detected after the onset of renal ischemia as the result of loss of intracellular potassium ions [11]. In addition, attenuation of intracellular potassium loss by means of K<sup>+</sup> channel blockage has been shown to reduce hypoxic renal injury [11]. Finally, an increase in tissue electrical bioimpedance has been considered a reliable indicator of anoxic cellular edema by the detection of the narrowing of extracellular space and closure of gap junctions [12]. Ischemic cell swelling results from inhibition of energy metabolism, and it has been considered to be one of the major causes of renal ischemic damage [13;14].

I/R injury is a well-known feature of renal dysfunction [15]. Functional, metabolic, and morphologic methods have shown that ischemic preconditioning pre-treatment protects the kidney from ischemic injury [16]. Nevertheless, the effectiveness of this preconditioning has proved to be highly dependent on protocol approach [16;17], so it seems that tissue parameter monitoring may also help to assess the suitability of the strategy. Direct changes brought about by kidney ischemic preconditioning on the parameters that we measured have not been studied previously. However, by use of nuclear magnetic resonance, Cochrane et al. [16] showed an improved recovery of post-ischemic intracellular tissue pH after preconditioning. In addition, in myocardial tissue, preconditioning pre-treatment has been shown to attenuate changes of electrical impedance during ischemia [18]. Furthermore, it has been suggested that the protective role of ischemic preconditioning in the heart is mediated by adenosine triphosphate (ATP) K<sup>+</sup>-sensitive mitochondrial and cell membrane channels opening [19].

This study evaluated the capability of implanted renal tissue microelectrodes for early detection of kidney ischemia and for monitoring changes caused by preconditioning pretreatment. We also explored the basis of the protective action of ischemic preconditioning. The results showed rapid changes in the three variables studied induced by kidney I/R. However, only the impedance values suggested a significant effect for preconditioning treatment, essentially during the reflow period.

### 5.1.2. Materials and methods

#### ▪ Electrodes

The electrical impedance at 1 kHz was measured by employing the silicon probe described in chapter 2.

Commercial miniaturized Ion Selective Electrodes (ISEs) and glass reference electrodes were acquired to measure pH and K<sup>+</sup> extra-cellular levels (references 800, 601 and 401 from Diamond General Development Corp., Ann Arbor, MI, USA). The response of these electrodes was checked in lab using known solutions before the *in vivo* experiments. Especial effort was made to test sensibility, linearity, cross-interferences and drifts for the expected measurement ranges (pH from 6 to 8 and K<sup>+</sup> from 1 to 40 mM).

Before each *in vivo* experiment, the sensitivity of the pH and K<sup>+</sup> ISEs had to be calibrated. Two isotonic solutions of known pH and K<sup>+</sup> concentration were used (solution 1: 1mM K, pH 8.78; solution 2: 4mM K, pH 6.74) prepared from a NaCl buffer as described in [20]. The ISEs were kept in these calibration solutions for more than an hour in order to reduce the stabilization time after the insertion into the living tissue. As it is described later, baseline arterial plasma pH and K<sup>+</sup> measurements were used to set the time-zero values of tissue pH and K<sup>+</sup>.

#### ▪ Electronic instrumentation

It was necessary to develop a custom made instrumentation system<sup>3</sup> in order to measure multiple channels and multiple parameters (pH, K<sup>+</sup> and impedance).

**Table 5.1.** Instrumentation system main features

<hr/> Bio-impedance meter <hr/>	
Number of channels	10
Ground isolation impedance	50 pF
Oscillator frequency	100Hz to 125 kHz
Injected current amplitude	<5μA
CMRR at 1kHz	88 dB
Input common impedance	> 50 MΩ // 7pF
Input differential impedance	> 50 MΩ // 2pF
<hr/>	
Ion meter (voltmeter)	
Number of channels	16
Ground isolation impedance	50 pF
Input impedance	> 10 TΩ
<hr/>	

---

<sup>3</sup> See annex C.2.1 for further details.

- Validation of the measurement frequency

At frequencies below 1 Hz and at low current densities, the electrical bioimpedance is mainly related with the extracellular medium since the cell membranes behave as dielectric layers with very low conductance. In the case that the conductivity of the extracellular medium do not changes significantly, this fact can be exploited to study the extracellular volume changes. Unfortunately, due to the electrode-electrolyte interface impedance, it is impractical to work at these frequencies without important measurement errors. In some cases, however, it is possible to use higher frequencies and consider that the results are very close to those obtained at a very low frequency. Generally, 1 kHz is considered to be a sufficiently low frequency to study the extracellular medium [21] because, at this frequency, most of the current does not penetrate into the cells. At the same time, this frequency is not too low to induce measurement errors because of the electrode-electrolyte interface impedance. Thus, *a priori* this frequency seemed a proper choice, but, taking into account the singularity of the tissue under study in the related experiments, impedance spectroscopy was used to test the suitability of this frequency. It was tested to check if at this frequency it would produce results similar to those obtained from studies at lower frequency (~ 1 Hz). The test is based on the fact that most living tissues exhibit relaxation processes that can be modeled by the Cole equation<sup>4</sup>, and from that model it could possible to obtain an impedance value at 0 Hz ( $R_0$ ):

$$\mathbf{Z} = R_{\infty} + \frac{\Delta R}{1 + (j\omega\tau)^{\alpha}} \quad , \quad \Delta R = R_0 - R_{\infty} \quad (5.1)$$

Following the same procedures that are described in the next sections, the right kidney of a rat was subjected to acute ischemia (60 min.) followed by a reperfusion period (25 min.) while the impedance was monitored using the needle probe and the SI1260 + front-end system (see annex C.2.3). The impedance values were obtained from 10 Hz to 1 MHz at every 50 seconds. With the resulting data, the Cole parameters for the low frequency relaxation were automatically fitted with *ad hoc* developed Matlab™ routines. Then, after verifying a good Cole fitting, it was possible to compare the  $R_0$  value with impedance magnitude at higher frequencies.

- Animals and Anesthesia

The study was conducted under the supervision of the IIBB ethics commission and conformed to European Union guidelines for the handling and care of laboratory animals. Male Wistar rats (Ifa Credo, Spain), weighing 250 to 300 g, were anesthetized with sodiumpentobarbital (50 mg/kg). Supplemental boluses were administered during each experiment. Polyethylene cannulas (PE-50, Clay Adams, Sparks, MD) were inserted through the left carotid artery into the aorta for blood sampling and saline infusion (1 ml/100 g/hr). A tracheotomy was performed, the trachea was intubated (polyethylene tubing, PE-240), and ventilation was maintained using a Harvard animal

---

<sup>4</sup> See annex A

respirator. We kept PaCO<sub>2</sub> values between 4.5 and 6 kPa using ventilatory control, whereas PaO<sub>2</sub> was maintained between 15 and 20 kPa by adequate oxygen-air control of gas mixture supply. The abdominal area was covered with saline wet gauze at 37°C and a plastic cover to minimize dehydration of exposed tissues. Animals were permanently exposed to radiant heat, and deep abdominal and kidney surface temperatures were maintained at 36°C to 37°C (thermocouple probes KP1/45, Kane May, London UK). Arterial blood samples (0.15 ml) were obtained initially and during the reflow periods for gasometric control and measurement of arterial pH and plasma [K<sup>+</sup>] (BMS3 MK2 Blood Microsystem and EML100 Electrolyte Metabolite Laboratory, Radiometer, Denmark).

- Experimental Protocol

To induce kidney I/R, laparotomy was performed, and the left renal pedicle was dissected and occluded with a nontraumatic microvascular clamp. Rats were randomized into three groups. A minimum of n=5 valid whole data set per parameter required six to eight animals per group as the result of fall-out of some measurements.

The three groups were as follows: sham-operated controls (C); 45 min left renal ischemia, followed by 60 min reperfusion (I/R); and 45 min left renal ischemia, followed by 60 min reperfusion, preceded by ischemic preconditioning of 10 min of ischemia and 10 min of reperfusion (IP).

The bioimpedance probe was inserted into the kidney by direct puncture. Bleeding was negligible. Effectively measuring impedance volume predominantly included the medullar region (inner electrodes laid in the medulla and the outer ones in the joint area between the medulla and the cortex). ISE probes were inserted intrarenally at a depth of approximately 2 mm, with the help of a cutting edge needle allowing controlled deep puncture. Bleeding was minimal, and the tip of the electrodes lay in the boundary between the medulla and cortex. The reference electrode was laid into the abdominal cavity. Electrodes were held by supports and the insertion was maintained constant.

### 5.1.3. Results

- Validation of the measurement frequency

After inducing ischemia by arterial clamping, R<sub>0</sub> increased from 1.7 kΩ to 12.5 kΩ in 60 min. The impedance magnitude at 1 kHz followed this evolution with a reduced sensitivity resulting in a 25 % of maximum relative difference. This fact could suggest the use of lower frequencies to reduce this difference, however, it must be taken into account that measurement artifacts were observed for frequencies below 300 Hz and that the range of possible interface impedances is amazingly wide. Therefore, in order to ensure quality for all the measurements it seems that 1 kHz is a proper choice.

Figure 5.1 shows the results obtained from this experimental test before and after 10 minutes of induced ischemia and the superimposed Cole fittings. The Cole models were adjusted for low frequencies (<10 kHz) since the relaxation arc presented distortion for higher frequencies due to other tissue relaxation constants and because of the needle parasitic capacitances.

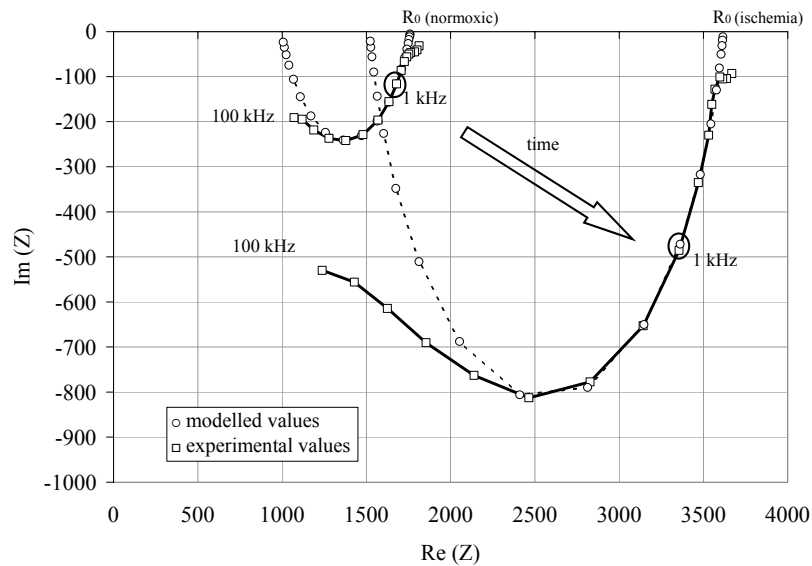


**Figure 5.1.** Nyquist plot evolution from a kidney rat subjected to ischemia (frequency sweeping plots before and after 10 minutes of induced ischemia). The modeled values ( $\circ$ ) have been adjusted to the experimental values ( $\square$ ) for the arc observed at low frequencies.

- Series of *in vivo* tests

Plots are shown for tissue pH values (Figure 5.2), interstitial potassium ion concentration (Figure 5.3), and impedance magnitude (Figure 5.4). Baseline arterial plasma pH and  $[K^+]$  measurements were used to set zero-time values of tissue pH and  $[K^+]$ . Arterial blood gas composition was controlled, and no significant changes in acid-base status were found at any time during the experiments.

#### *Ischemia*

Renal vascular occlusion induced immediate, rapid changes in the variables monitored: a decrease in pH and an increase in  $[K^+]$  and impedance. Significant differences from baseline values were found for three variables after 5 min of ischemia. Rapid initial changes in the three parameters were followed by a rate decrease as ischemia progressed.

### Reperfusion

Vascular clamp release increased kidney pH, but the mean baseline levels were not recovered during the experiment (Figure 5.2).  $[K^+]$  decreased rapidly; this was the only parameter in the ischemic group that returned to baseline values during the reflow period (Figure 5.3). Postischemic impedance decreased sharply, reaching a minimum within the first 10 min of reperfusion, but then increased for the second time, reaching new peak values after approximately 20 min of reperfusion, before a slow decrease (Figure 5.4).

### Effect of Preconditioning

Ischemic preconditioning did not significantly influence pH and  $[K^+]$  values during I/R (Figure 5.2 and Figure 5.3) whereas preconditioned kidneys reached higher impedance mean values (Figure 5.4). Furthermore, during reperfusion, preconditioning significantly decreased impedance values, eliminating the postischemic increase of impedance found in nontreated rats (Figure 5.4).

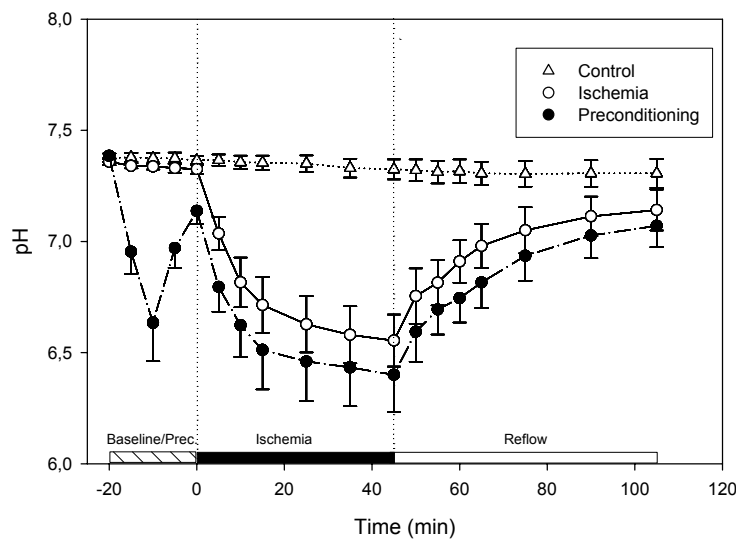


**Figure 5.2.** Extracellular pH in the three groups (control group, ischemia-reperfusion group and preconditioned + ischemia-reperfusion group). pH mean values  $\pm$  SEM.



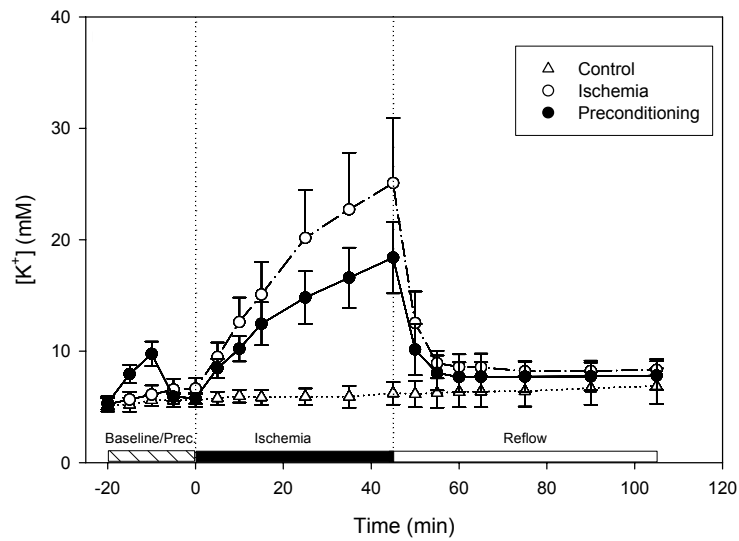


**Figure 5.3.** Extracellular potassium ion concentration in the three groups (control group, ischemia-reperfusion group and preconditioned + ischemia-reperfusion group). [K<sup>+</sup>] mean values  $\pm$  SEM.

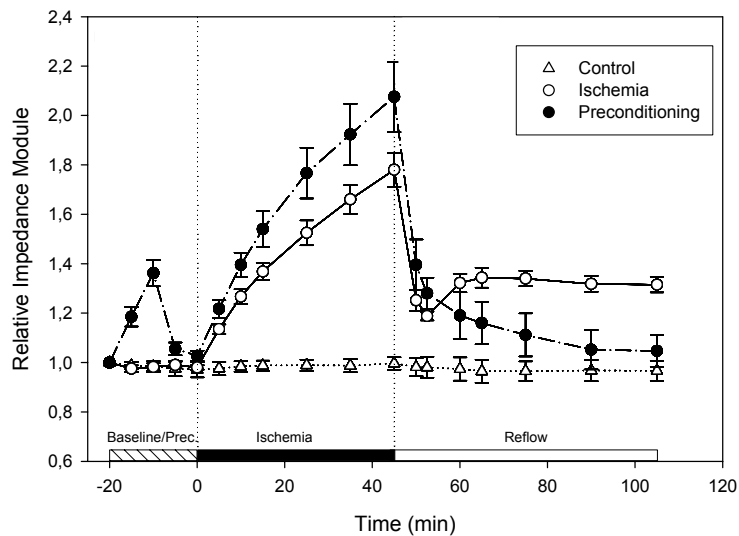


**Figure 5.4.** Relative impedance magnitude (referred to baseline) in the three groups (control group, ischemia-reperfusion group and preconditioned + ischemia-reperfusion group). Impedance magnitude mean values  $\pm$  SEM.

#### 5.1.4. Discussion

Understanding the effects of I/R injury is important and increasingly relevant with the use of marginal organs, particularly organs from non-heart-beating donors. The use of microelectrodes to monitor the effects of ischemia is clearly an important way of studying the critical events that take place and, possibly, establishing which organs are

likely to remain viable. Although experiments have shown that pH and PCO<sub>2</sub> electrodes placed at the surface of the kidney are able to detect renal cortical ischemia [9;10], no current method exists for reliable monitoring of kidney ischemia. The use of microsensor technology for real-time measurement of intraorgan tissue parameters may lead to possible clinical applications in the near future, as smaller probes and more advanced telemetric monitoring technology become available.

This article discusses the changes induced by kidney I/R and ischemic preconditioning treatment on three renal tissue parameters, which all register changes soon after the onset of ischemia and thus may be good candidates for detecting ischemia and monitoring its therapeutic management.

The impedance probes used in most past studies are excessively invasive for intraorgan small-volume measurement, as is required in the rat kidney. In this study, these problems were overcome by the use of a novel miniature silicon needle. Unlike ISEs, which measure tissue properties just at the electrode tips, bioimpedance measurements are representative of a tissue volume around the electrodes and, therefore, are not so influenced by the transient tissue changes caused by the puncture.

#### *Changes Monitored During Ischemia-Reperfusion*

Each variable monitored during ischemia showed an immediate change, followed by a decreased rate change with time. Whereas impedance magnitude and [K<sup>+</sup>] continued to increase during late ischemia, pH reached a minimal plateau phase. This difference in evolution over time can be attributed to the different underlying mechanisms of the ischemia-induced changes. Lack of oxygen causes intracellular pH to decrease as the result of glycolytic lactic acid generation and ATP depletion processes [8]. Metabolic influence also seems apparent in the evolution of [K<sup>+</sup>] and impedance. However, [K<sup>+</sup>] and impedance changes beyond the time point where pH reaches the plateau phase indicate that passive ion and water shifts occur after ATP depletion [22]. Significant tissue cellular ATP depletion has been found within the first minutes of renal ischemia [23], and in other studies, ATP and intracellular pH values remained stable beyond 25 min of ischemia [16]. Our results showing extracellular pH evolution are in agreement with these changes.

Among the factors that may contribute to rapid increase of interstitial potassium after the onset of ischemia, dysfunction of the sodium-potassium pump as the result of ATP depletion [22], activation of potassium channels [11], and water shifts to intracellular compartment [22] should be considered. In the kidney, as in other tissues, one of the earliest ischemic events is a loss of intracellular K<sup>+</sup> [11]. Renal ischemia increases the open probability of the K<sup>+</sup> ATP channels independently of pump activity [24]. Our results indicate that the activation of potassium channels is an early response to hypoxia, and that K<sup>+</sup> efflux must be independent of active K<sup>+</sup> uptake, because the extracellular K<sup>+</sup> rate increase is still pronounced in the late ischemic phase (Figure 5.3).

During ischemia, we found a progressive increase of bioimpedance measured at low frequency. This rise is considered to reflect the occurrence of an anoxic edema as the result of cell swelling, which leads to a reduction of extracellular space, an increase in extracellular resistance, and cell-to-cell uncoupling [12] in organs with gap junctions such as the kidney. Tissue edema has been reported to be one of the major causes of renal ischemic damage [13;25]. The prompt, rapid onset of intrarenal impedance changes, with a maximum rate of increase after renal artery occlusion, contrasts with the sequential changes described in myocardial impedance [18]. Our study found a second increase in impedance values during reperfusion. This increase may indicate the occurrence of intracellular edema during reflow, probably linked with the no-reflow phenomenon, that is, the absence or reduction of vascular reflow after relief of kidney ischemia [25]. Decreases in renal blood flow of 30% and 50% have been measured in rats and dogs, respectively, after 30 min of reperfusion after 30 and 60 min of renal artery clamping [13;26].

#### *Ischemic Preconditioning Influence on Ischemia-Reperfusion Measured Parameters*

The evolution of monitored intrarenal parameters supports the idea that the mechanisms underlying the protective actions of ischemic preconditioning vary according to organ [7], particularly between heart and kidney [16]. In our study, ischemic preconditioning did not reduce ischemic acidosis, as has been reported for myocardial ischemia [27]. Although severe intracellular acidosis is considered a cause of injury in ischemic myocardial tissue [16], acidic tissue pH during I/R may have a protective effect in kidney and other tissues [28]. Measuring intracellular pH (pHi) by means of nuclear magnetic resonance spectroscopy, Cochrane et al. [16] also found that pHi decreased to a similar degree in preconditioned and control kidneys during ischemia; however, pHi recovery during reflow improved in preconditioned kidneys. Our result, the absence of any improvement in tissue pH recovery in preconditioned kidneys during reperfusion, does not necessarily contradict Cochrane et al.'s finding. Tissue-implanted microelectrodes measure extracellular pH, and the improved recovery of intracellular pH in preconditioned kidneys with no changes in extracellular pH could be attributed to the enhanced activity of membrane acid-base equivalent exchangers in the postischemic period.

We also report that preconditioning did not increase extracellular potassium during ischemia. Therefore, our results do not favour the idea of a protective pathway of preconditioning in the kidney through the opening of ATP-sensitive potassium channels, as has been proposed for myocardial tissue [19;29;30]. In the ischemic kidney, it has been postulated that the activation of potassium channels contributes to hypoxic injury in proximal tubules [11]. Furthermore, contrary to what has been suggested for myocardial tissue, attenuation of potassium loss during hypoxia by channel blockage protects against hypoxia-induced injury [11].

Surprisingly, we found higher tissue impedance values in the late ischemic phase of preconditioned kidneys. In contrast with its effect on myocardial tissue, ischemic preconditioning did not postpone or attenuate the ischemic tissue resistivity increase in kidney [18;19]. These results indicate that the preventive effect of kidney ischemic

preconditioning cannot be attributed to a reduction of hypoxic intracellular edema. Indeed, kidney preconditioning may be effective despite the increased bioimpedance values found. In this regard, the results of a study on differential effects of swelling and anoxia (60 min warm ischemia) on kidney function showed that nonanoxic edema is much less damaging than anoxia, and that ischemic injury in kidney was not the simple consequence of the spatial disruption of cell architecture [13].

The most interesting effect of ischemic preconditioning found here was a significant reduction of postischemic tissue impedance. This may indicate that preconditioning decreases cellular edema during the reflow period. Further information supports this [26], showing that ischemic preconditioning protects against I/R-mediated kidney injury by improving renal blood flow during reperfusion. The same action, described in other tissues such as the small bowel, has been associated with an improvement of tissue injury and metabolism [31].

#### **5.1.5. Conclusions**

Our results show that intrarenal microelectrode real-time measurement of any of the three variables studied is a suitable technique for early detection of ischemia in the kidney. Tissue-impedance monitoring using a single microprobe showed the occurrence of reperfusion cellular edema. The improvement in reflow tissue bioimpedance was the most noticeable beneficial effect of ischemic preconditioning. Some physiologic conclusions of interest, regarding the actions of preconditioning, can be drawn from the negative results obtained. Evidence is given to suggest that, unlike the heart, the protective action of preconditioning in the kidney does not seem to be mediated by the opening of potassium channels, decreased tissue acidosis, or improved tissue impedance properties during the ischemic period.

## 5.2. Electrical bioimpedance measurement during hypothermic rat kidney preservation for assessing ischemic injury.

Non-heart-beating donors sustain an ischemic insult of unknown severity and duration, which can compromise the viability of the graft. This preliminary study aimed to assess whether electrical bioimpedance monitoring of cold preserved organs could be useful to identify kidneys that have suffered previous warm ischemia (WI). Two rat kidney groups were studied during 24 hours of preservation in University of Wisconsin solution (UW): a control cold ischemia group and another group subjected previously to 45 minutes of WI. Multi-frequency bioimpedance was monitored during preservation by means of a miniaturized silicon probe and the results were modeled according to the Cole equation. Tissular ATP content, lactate dehydrogenase in UW solution and histological injury were assessed. Renal function and cell injury, evaluated during 3 hours of *ex vivo* reperfusion using the isolated perfused rat kidney model, demonstrated differences between groups. Bioimpedance results showed that the time constant and the high frequency resistivity parameters derived from the Cole equation were able to discriminate between groups at the beginning of the preservation ( $\Delta\tau \sim 78\%$ ,  $\Delta R_\infty \sim 36\%$ ), but these differences tended to converge as preservation time advanced. Nevertheless, another of the Cole parameters,  $\alpha$ , showed increasing significant differences until 24h of preservation ( $\Delta\alpha \sim 15\%$ ).

This work is presented in:

- Genescà, M., Ivorra, A., Sola, A., Palacios, L., Goujon, J. M., Hauet, T., Villa, R., Aguiló, J., and Hotter, G., "Electrical bioimpedance measurement during hypothermic rat kidney preservation for assessing ischemic injury," *Biosensors & Bioelectronics*, vol. Accepted for publication 2004.

### 5.2.1. Introduction

The use of non-heart-beating donor (NHBD) kidneys has been introduced in an attempt to reduce the gap between the supply and demand of organs for transplantation [32]. However, with the use of NHBD kidneys, where a prior insult of warm ischemia (WI) precedes the period of cold ischemic preservation (CI), delayed graft function and primary non-function increase in comparison to the heart-beating donor [33]. The extent of WI damage in these donors is difficult to determine on the basis of clinical data alone. Therefore, objective methods to evaluate the potential function of a renal graft upon transplantation would help to overcome this problem.

*Ex vivo* assessment of renal graft viability has focused on monitoring perfusion pressure/flow during hypothermic perfusion preservation or on measuring biochemical parameters, such as energy charge and release of alpha glutathione S-transferase [34]. Determination of most of these parameters requires the use of a

preservation machine, which is not routinely used. However, the gold standard for kidney evaluation is usually renal biopsy, which is invasive and frequently inconclusive.

Electrical bioimpedance (electrical impedance of biological samples) provides information on the physiological and morphological condition of living tissues [35] and has been suggested as an indicator of anoxic cellular edema and inter-cell uncoupling in cold preserved organs [12]. Since the consequences of ischemia such as cellular edema or cytoskeletal alterations are traduced in different morphological and structural changes [36;37], we hypothesized that electrical measurements could be a useful tool for organ evaluation in renal transplantation. Here we compare the behavior of multi-frequency impedance analysis parameters between two experimental groups, which characterize two different situations, relating the to functional parameters in the reperfused kidney.

### 5.2.2. Materials and methods

#### *Experimental groups and protocols*

A total number of 52 animals were randomly assigned into 2 different groups:

Group 1: Cold ischemia group (CI); kidneys were isolated and preserved for 24 hours in UW preservation solution.

Group 2: Warm ischemia group (WI); kidneys underwent a previous period of 45 minutes of warm ischemia before isolation and cold storage.

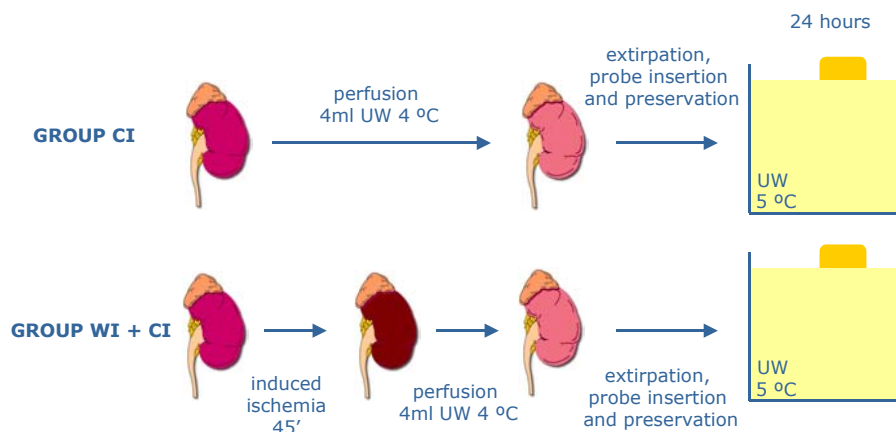


**Figure 5.5.** Experimental groups.

On-line monitoring of electrical bioimpedance during preservation (n=8 each group): Just before starting the preservation, the bioimpedance microprobe was inserted orthogonally in the kidney. The probe was placed close to the corticomedullar junction, the area in which the most pronounced injury has been found in ischemia-reperfusion. In small organs such as the rat kidney, since the electric field covers a high relative volume, the measurements may be considered representative of homogeneous tissue properties.

Study of histological parameters during preservation (n=4 each group): Kidneys were obtained at 24 h of preservation and fixed for histological evaluation.

Study of other viability markers during preservation (n=4 each time group): Kidneys and preservation solution samples were obtained at different preservation times (0, 2, 4, 8 and 24 h). Tissue samples were freeze-clamped to determine ATP content. The solution samples were also frozen to determine lactate dehydrogenase (LDH) accumulation into the solution.

Assessment of renal function in the IPK model (n=4 each group): Kidneys underwent 3 hours of *ex vivo* perfusion after the preservation period to assess renal function. Renal perfusion flow (RPF) was determined volumetrically every 30 minutes. Perfusate samples were taken at 3 hours of perfusion to determine creatinine and LDH activity.

#### ***Animals and anesthesia***

The study was performed using male Wistar rats (Ifa Credo, Barcelona, Spain) weighing between 250-300 g. Animals were anesthetized by intraperitoneal injection of sodium pentobarbital (30 mg/kg.) and placed in a supine position, keeping body temperature between 36 °C and 37 °C. All procedures were conducted under the supervision of our institution's Research Commission and followed EU guidelines for the handling and care of laboratory animals.

#### ***Surgical techniques***

The abdomen was opened by a midline incision. The right adrenal artery and the small lumbar arteries were tied off. Heparin (1000 U) was administered by intravenous puncture. Just after the occlusion of suprarenal aorta, a polyethylene catheter (PE-50) was inserted into the infra-renal aorta. The kidneys were immediately flushed *in situ* with 8 ml of University of Wisconsin (UW) preservation solution at 4 °C, at a maximum pressure of 60 mmHg. The left kidney was immediately removed, placed in a recipient with 20 ml of UW at 4 °C for 24 hours. Bath temperature was controlled by using an immersion cryostat (Frigiterm-10, Selecta, S.A., Spain). Right kidneys were used for the histological analyses.

In the case of WI group, warm ischemia was induced by suprarenal aortic cross clamping for 45 minutes previous to preservation.

#### ***Isolated perfused rat kidney (IPK) model***

The perfusion system followed the method described by Herrero et al. [38] with minor changes. After preservation, the kidney was placed in a perfusion chamber at a constant temperature (37.5 °C) and the renal artery cannula was connected to a recirculating system for 3h. The perfusion fluid (modified Krebs-Henseleit solution at 37 °C) was oxygenated with a 95% O<sub>2</sub>/5% CO<sub>2</sub> mixture. The perfusion pressure was kept constant at 60 mmHg.

### ***Biochemical analysis***

Nucleotide determination: Renal samples were processed by HPLC as previously described [39].

Creatinine determination in the renal perfusate was performed following the manufacturer's instructions (Sigma Chemical Co.; Madrid, Spain).

LDH activity determination: LDH assay kit (Roche Diagnostic Systems, Montclair, NJ).

### ***Histopathology evaluation***

Biopsies from the deep cortex-outer medulla region of the kidney were fixed in Bouin buffer solution and sections stained with hematoxylin-eosin and periodic acid-Schiff. Quantitative assessment was performed as described before [40]. Four basic morphological patterns typical of ischemic injury (interstitial edema, intracellular edema, cell detachment and brush border integrity) were graded on a five-point scale as follows: 1, no abnormality; 2, mild lesions affecting 10% of samples; 3, lesions affecting 25%; 4, lesions affecting 50%; 5, lesions affecting more than 75%.

### ***Bioimpedance monitoring and data processing***

Electrical bioimpedance was measured by using a miniaturized probe that consisted of four platinum electrodes ( $300\ \mu\text{m} \times 300\ \mu\text{m}$ ) on a needle shape silicon substrate [41].

The impedance measurement system consisted of a commercial impedance analyzer (SI1260, Solartron Analytical, Cambridge, UK), a custom made front-end to enhance the SI1260 input properties<sup>5</sup>, a switching matrix to select one of four channels and a computer that controlled the sub-systems and stored the data from the SI1260. The system was configured to perform frequency sweeps from 100 Hz to 100 kHz every 30 seconds and an oscillator voltage of 20 mV was selected, which meant that the maximum injected current was 7  $\mu\text{A}$ . An analysis of the probe frequency properties and a more detailed description of the instrumentation system can be found elsewhere [41].

The impedance spectrogram was characterized by the mathematical model described by the Cole equation (equation 5.1)

For each time sample, the parameters  $R_\infty$ ,  $R_0$ ,  $\tau$  and  $\alpha$  were adjusted to reproduce the impedance spectrogram. The fitting was automatically performed from the measurements at three specific frequencies (681 Hz, 2154 Hz and 14678 Hz) by finding the arc that comprises the  $(\text{Re}\{Z\}, \text{Im}\{Z\})$  points at the Nyquist plot for those frequencies.

After the fitting, the Cole parameters ( $R_\infty$ ,  $R_0$ ,  $\tau$  and  $\alpha$ ) were plotted (expressed as mean  $\pm$  standard error of the mean) and studied in order to identify the ones that distinguished best between the groups. Special attention was paid to certain time points (0, 2, 4, 8 and 24 hours). The  $R_\infty$  and  $R_0$  parameters were scaled according to the

---

<sup>5</sup> See section C.2.3



probe cell constant and their values were expressed as resistivities ( $\Omega\cdot\text{cm}$ ) instead of resistances ( $\Omega$ ).

### *Statistical analyses*

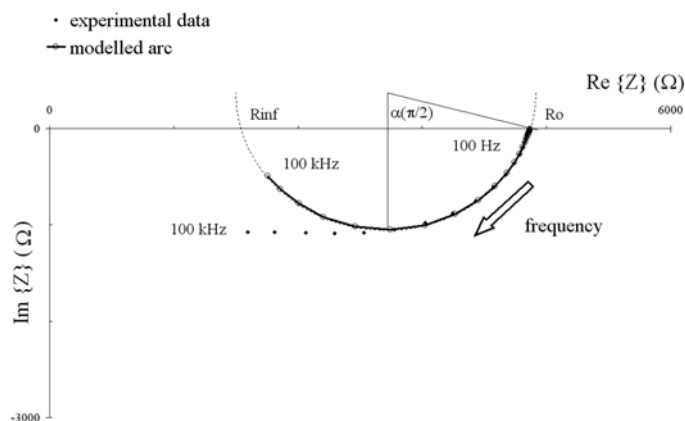
Data are expressed as means  $\pm$  SEM. Means of different groups were compared using variance analysis and the Student-Newman-Keuls test for multiple comparison. When a non-parametric test was needed, the Kruskal-Wallis analysis was used. Significant results were determined by  $P < 0.05$ .

### 5.2.3. Results

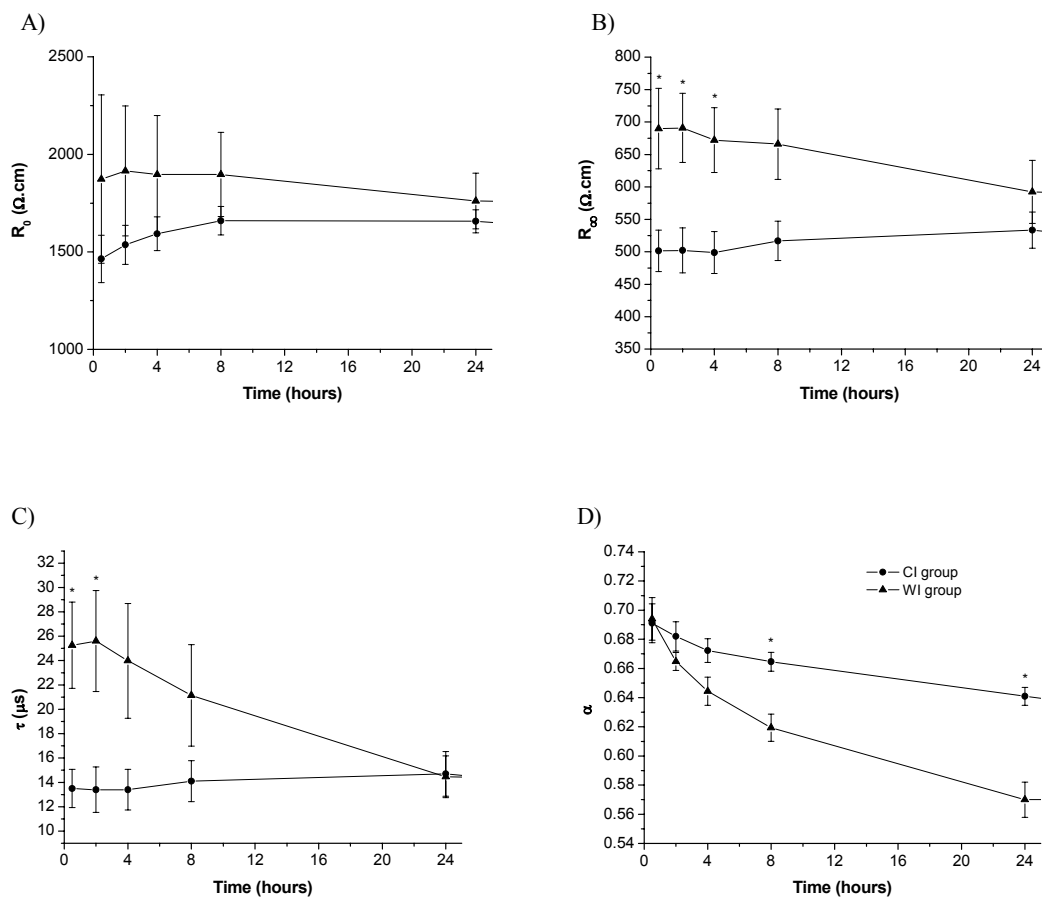
#### *Bioimpedance monitoring during cold ischemia*

Figure 5.6 shows an example of the data measured by the impedance measuring system at a specific time point (CI group at 0.5 hours). The multi-frequency measurements produce an arc in the Nyquist plot (real part of impedance versus imaginary part of impedance) that is compatible with the Cole model for a single dispersion. At frequencies higher than 15 kHz, the response differed from the Cole model. This could indicate a second superimposed dispersion. However, we do not take it into account due to the impedance probe limitations at high frequencies [41].

The shape of the arc and, consequently, the four Cole parameters clearly evolved across preservation time (Figure 5.7). Both groups produced different bioimpedance responses, with the most significant differences being found for parameters  $\tau$  and  $\alpha$ . The parameter  $\tau$  clearly differentiated between CI and WI+CI groups at the beginning of the preservation and tended to converge at the end of the preservation (Figure 5.7C). On the other hand,  $\alpha$  parameter differentiates the groups after the first 6 hours and continues until 24 h (Figure 5.7D). The parameters  $R_0$  and  $R_\infty$  also differentiated between groups but their deviation was excessively large (Figure 5.7A and Figure 5.7B).



**Figure 5.6.** Example of impedance locus at 0.5 hours. The modeled arc is superimposed on the actual data.



**Figure 5.7.** Cole parameters (A)  $R_0$  ( $\Omega \cdot \text{cm}$ ), (B)  $R_\infty$  ( $\Omega \cdot \text{cm}$ ), (C)  $\tau$  ( $\mu\text{s}$ ) and (D)  $\alpha$  (adimensional) at different times (0.5, 2, 4, 8, and 24 hours) during cold preservation. CI: cold ischemia; WI+CI: warm ischemia + cold ischemia. \*  $P < 0.05$  WI+CI vs CI.

### Assessment of biochemical markers and histological analysis during preservation

Table 5.2 shows the histological evaluation, the ATP tissular content and LDH accumulation in the preservation solution. The semi-quantitative scores for the morphological parameters studied demonstrate, as expected, a slightly higher degree of cellular damage in proximal tubule cells in the group with previous ischemia (WI+CI) comparing to CI group. Nevertheless, these differences in intracellular edema, interstitial edema, loss of brush border and cell detachment were not clear enough to differentiate between groups.

ATP content and LDH accumulation were measured at different selected preservation times (data shown only at 24h preservation time point, Table 5.2). The WI+CI group showed a significant decrease in ATP renal levels at the beginning of the preservation period (0 hours) compared with CI group ( $481.4 \pm 58$  vs  $680.0 \pm 60.0$ ). This difference between the groups was significant again at 8 and 24 hours of preservation ( $406.8 \pm 60.9$  vs  $745.3 \pm 26.0$  and  $409.5 \pm 11.5$  vs  $594.6 \pm 26.2$  respectively). LDH accumulation in the

preservation solution showed a tendency to present greater values in LDH release during all the preservation time in the WI+CI group compared with CI group, nevertheless these differences were not significant.

**Table 5.2.** Evaluation of proximal tubule cell injury (graded on a five-point scale), ATP tissular levels and LDH accumulation into the solution at 24 h of preservation.

Group	CI	WI+CI
Intracellular Edema	1.2 ± 0.5	1.7 ± 0.5
Interstitial Edema	2.0 ± 0.0	2.0 ± 0.2
Loss of brush border	1.5 ± 0.3	2.0 ± 0.0
Cell detachment	1.5 ± 0.3	2.0 ± 0.0
Mean score ± SEM	1.55 ± 0.19	1.92 ± 0.08
LDH accumulation (U/ml)	0.52 ± 0.015	0.59 ± 0.049
tissular ATP (pmol/mg)	594.6 ± 26.2	409.5 ± 11.5*

Values are expressed as means ± SEM.

\* P <0.05 WI+CI vs

#### ***Functional and injury markers during reperfusion***

The mean values for creatinine and LDH in the perfusate at 3 h of reperfusion were significantly higher in the WI+CI group compared to CI group (Table 5.3). Perfusion of the isolated kidneys showed strong differences between the groups in RPF, from 60 minutes of perfusion until the end of the experiment (180min).

**Table 5.3.** LDH, creatinine and RPF at 3 hours of reperfusion in isolated perfused kidneys.

Group	LDH (U/ml)	Creatinine (mg/dl)	RPF (ml/min/g)
CI	0.015 ± 0.010	0.999 ± 0.041	9.20 ± 0.29
WI+CI	0.146 ± 0.081*	1.132 ± 0.035*	5.80 ± 0.72*

Values are expressed as means ± SEM.

\* P <0.05 WI+CI vs CI.

#### **5.2.4. Discussion**

It has been widely reported that the use of NHBD kidneys, where a prior insult of WI precedes the period of CI preservation, is clearly associated with an increase in delayed graft function and primary non-function when compared with organs from heart-beating donors [33]. Therefore, the previous ischemic process that a particular organ has undergone may have a dramatic effect on the end result of transplantation. So far, no currently used biochemical or histological parameters are conclusively related to graft viability. In our study, histological evaluation revealed slight differences in interstitial edema and proximal tubule cell injury between CI and WI+CI groups at the end of preservation, but these differences were not enough clear to discriminate between groups. However, the functional parameters measured after 3 hours of reperfusion in IPK model reflected differences existing between groups. WI+CI kidneys are functionally impaired in reperfusion, as shown by PFR and creatinine, and also present tubular injury, as demonstrated by LDH release.

Measurements of alternatively biochemical markers such as LDH and ATP content during preservation storage showed differences between groups. Regarding LDH accumulation into the preservation solution, there was only a tendency in the differences, suggesting greater cellular damage in WI+CI group. In the case of tissular ATP content, this measurement clearly discriminated between groups, in accordance with other studies [34] after 8 hours of preservation. However, the problem with ATP determination in renal tissue is that requires biopsy and is not rapid enough to be performed previously to the transplant procedures.

The hypothesis of the present work was that since the consequences of ischemia such as cellular edema or cytoskeletal alterations (loss of brush border, formation of apical blebs, cellular detachment, etc.) are traduced in different morphological and structural changes [36;37], and these changes in tissular structure can modify the electrical properties of the tissue, the measurement of electrical impedance could be the basis for a rapid and useful tool for organ evaluation in renal transplantation. That is, the objective was to assess whether or not electrical bioimpedance could become an alternative to current histological and biochemical parameters.

Although the relationship between the physiological causes and the effects on impedance is not direct, and different physiological causes can induce the same impedance response and *vice versa* [42], a relationship between physiological and bioimpedance tissue features is generally accepted during ischemia;  $R_0$  has been related with intra-cellular edema [35]: the ischemic cell swelling resulting from inhibition of energy metabolism [25] narrows the extra-cellular space and, consequently, reduces the width of the electrical path for low frequency currents, thus decreasing conductance, increasing resistance and thus increasing  $R_0$ . The evolution of  $R_0$  in Figure 5.7A shows that in the CI group, values tended to increase during the first 24 hours of preservation. In contrast, the WI+CI group, which started from higher  $R_0$  values due to the effect of the previous WI did not show this increasing pattern, although it maintained higher values than the CI group. A possible explanation of this WI+CI group evolution is, that after WI, there is a major ionic imbalance (especially for  $\text{Na}^+$ ) between the intra and the extra-cellular media causing an increase in intra-cellular osmotic pressure and cell swelling [22]. When the kidney is immersed in the UW solution, cell shrinkage occurs and, consequently,  $R_0$  decrease results as a consequence of hyper-osmolarity of UW and extra-cellular ionic shifts.

The  $\tau$  parameter differentiates clearly between the groups during short preservation times. It has been described that the parameter  $\tau$  is related to the cell membrane capacitance (C) and the intra and extra-cellular conductivities. Some authors have concluded that during cellular edema the membrane capacitance increases due to the increase in the membrane surface [43;44]. This explanation agrees with the increase in  $\tau$  values found in the WI+CI at the beginning of preservation, indicating that intra-cellular edema process takes place as a consequence of WI.

The most significant result is that the  $\alpha$  parameter (Figure 5.7D) showed marked differences between groups during preservation and those differences were markedly increased according to the preservation time. The physical meaning of  $\alpha$  is not clearly understood. That is, there is not an agreement on the cause of  $\alpha < 1$ . It seems that  $\alpha$  follows some sort of induced damage that has nothing to do with the cellular edema. We do believe that  $\alpha$  may be related with the morphology<sup>6</sup> of the extra-cellular spaces. We suggest that  $\alpha$  could be used as a measure of the 'tortuosity' of the extra-cellular spaces.

### 5.2.5. Conclusions

In the present study we show that the use of the Cole parameters allow clear differentiation between two groups that show different behavior in the reperfusion. As the main novel finding of this preliminary study, we show that the evolution of  $\alpha$  is an easy and objective continuous real-time parameter to detect ischemic damage during rat kidney preservation and could be a promising method to assess graft viability in the future if further studies corroborate this findings in species closer to humans (currently underway). It must be noted that  $\alpha$  is a parameter often ignored in the electrical characterization of materials, not only in living tissues but also in the cases of biological membranes or cell cultures. However, as it has been shown here,  $\alpha$  allows the visualization of some facts that are not manifested by other electrical parameters. We do believe that  $\alpha$  should be analyzed in biosensors based on impedance measurements. Particularly, we suggest its introduction in the Electric Cell-Substrate Impedance Sensing (ECIS) field [46].

---

<sup>6</sup> The original paper [45] contains a larger explanation of  $\alpha$  and a computer simulation to reinforce this hypothesis. Here such information has been included in the next experimental section.

### 5.3. Bioimpedance dispersion width as a parameter to monitor living tissues. Impedance spectroscopy and cytoskeleton disruption

In the case of living tissues, the spectral width of the electrical bioimpedance dispersions (closely related with the  $\alpha$  parameter in the Cole equation) evolves during the ischemic periods. This parameter is often ignored in favour of other bioimpedance parameters such as the central frequency or the resistivity at low frequencies. The object of this paper is to analyze the significance of this parameter through computer simulations (in the  $\alpha$  and  $\beta$  dispersion regions) and to demonstrate its practical importance through experimental studies performed in rat kidneys during cold preservation. The simulations indicate that the dispersion width could be determined by the morphology of the extra-cellular spaces. The experimental studies show that it is the unique parameter able to detect certain conditions such as a warm ischemia period prior to cold preservation or the effect of a drug (Swinholide A) able to disrupt the cytoskeleton. The main conclusion is that, thanks to the  $\alpha$  parameter in the Cole equation, the bioimpedance is not only useful to monitor the intra/extracellular volume unbalances or the inter-cellular junctions resistance but also to detect tissue structural alterations.

This work is presented in:

- Ivorra, A., Genescà, M., Hotter, G., and Aguiló, J. "Bio-impedance dispersion width as a parameter to monitor living tissues". 87-90. 2004. Gdansk, Poland. Proceedings from the XII International Conference on Electrical BioImpedance (ICEBI). 20-6-2004.
- Ivorra, A., Genescà, M., Sola, A., Palacios, L., Villa, R., Hotter, G., and Aguiló, J., "Bioimpedance dispersion width as a parameter to monitor living tissues," *Physiol Meas.*, vol. 26 pp. (accepted for publication), 2005.

#### 5.3.1. Introduction

One of the first successful electrical models for the electrical passive properties of living tissues was introduced by Fricke and Morse in 1925 [47]. It consists of a resistance for the extra-cellular electrolytic medium ( $R_e$ ) in parallel with the series combination of a resistance for the intra-cellular electrolytic medium ( $R_i$ ) and a capacitance for the cell membrane ( $C_m$ ). This model represents one relaxation process with a single characteristic time constant and, in the frequency domain, corresponds to a single dispersion, that is, a transition between two frequency-independent levels (see [35] for more details about these concepts).

The Fricke-Morse model has been extensively used and, even today, some authors make use of it [43;44] because of its simplicity and because it is able to describe qualitatively the observed main dispersion in the  $\beta$  dispersion region as defined by Schwan [48]. However, since the first studies, it was observed that this capacitive

model was not accurate enough to fit the experimental results in cell suspensions or living tissues studies [47]. When the impedance values measured at multiple frequencies are represented in a Bode plot, it is observed that the slope of the capacitive model is larger than the slope of the results from the actual bioimpedance characterization. Moreover, in the Nyquist plot (imaginary part versus real part) both, the capacitive model and the experimental results, produce a semicircle but, in the case of the actual data the center is not on the real axis. This phenomenon is usually described as ‘depressed semicircles’

In 1940 Keneth S.Cole [49] introduced the first mathematical expression able to describe the ‘depressed semicircles’ found experimentally. It is known as the Cole equation (here expressed as in [35]):

$$\mathbf{Z} = R_{\infty} + \frac{\Delta R}{1 + (j\omega\tau)^{\alpha}}, \quad \Delta R = R_0 - R_{\infty} \quad (5.2)$$

where  $Z$  is the impedance value at frequency  $\omega$ ,  $j$  is the complex number  $(-1)^{1/2}$ ,  $R_{\infty}$  is the impedance at infinite frequency,  $R_0$  is the impedance at zero frequency,  $\tau$  is the characteristic time constant and  $\alpha$  is a dimensionless parameter with a value between 0 and 1. Figure 5.8 shows the impedance magnitude and phase from the Cole equation for different values of  $\alpha$ . Note that  $\alpha$  is closely related with the spectral width of the dispersion, the minimum spectral width corresponds to  $\alpha = 1$  and the dispersion is broadened as  $\alpha$  tends to lower values. For that reason, here ‘dispersion width’ and  $\alpha$  are used indistinctively.

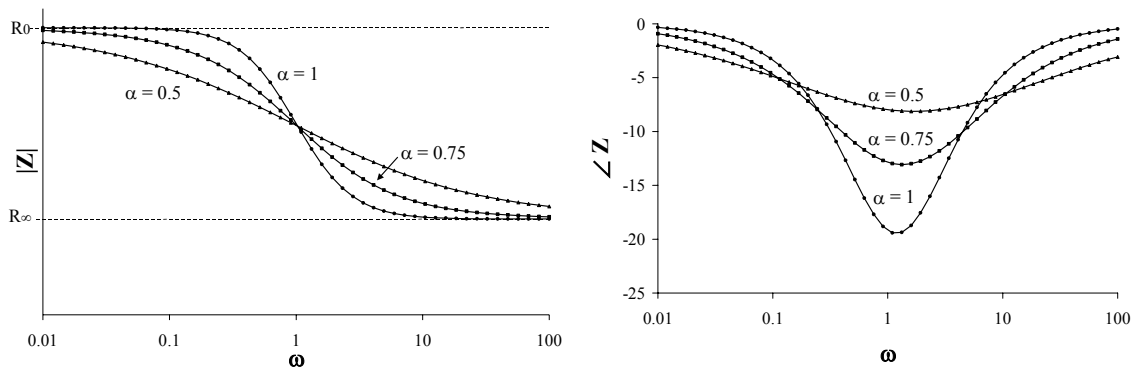


**Figure 5.8.** Impedance magnitude and phase angle from Cole equation for three  $\alpha$  values.

Living tissues usually exhibit one or two dispersions in the  $\alpha$  and  $\beta$  dispersion regions (from 1 Hz to some tens of MHz) that can be well approached by series combinations of (5.2). In those cases, the  $\alpha$  values are around 0.8 (note that  $\alpha$  in the Cole equation has nothing to do with the ‘ $\alpha$  dispersion region’). The physical phenomenon underlying each dispersion is generally understood. For instance, the large dielectric dispersion appearing in the  $\beta$  dispersion region is considered to be associated with the dielectric

properties of the cell membranes and their interactions with the extra and intra-cellular electrolytes. However, the physical meaning of  $\alpha$  is not clearly understood. That is, there is not an agreement on the cause of  $\alpha < 1$ . Most authors suggest that it is caused by the heterogeneity of cell sizes and shapes in a living tissue [50;51]. This explanation is based on the fact that a random distribution of relaxation times (time constants) with a certain probability density function will indeed produce an impedance spectrogram compatible with the Cole equation. Therefore it seems reasonable to think that the heterogeneity of an actual tissue could produce such a random distribution. However, to produce  $\alpha$  values around 0.8 it would be necessary a very broad distribution of relaxation times that cannot be related to the actual heterogeneity of tissues in terms of cell sizes and shapes. Hence the presence of mitochondrias and other compartments in the cell has also been suggested as a explanation to the broad distribution of relaxation times [52]. Among the other proposed theories [35] it must be mentioned the fractal interpretation of the dispersion broadening phenomenon postulated by Dissado [53]. He showed that the hierarchical organization of biological tissues can justify the frequency power law dependency of the dielectric response of animal tissues.

However, none of these theories can explain the fact that homogeneous clusters of cells without any hierarchical organization show the Cole behavior. Moreover, the above theories do not easily explain the fact that  $\alpha$  evolves with time under certain circumstances [21;54]. Our experiments on cold preservation of rat kidneys (see the experimental study section 5.2) show such a behavior and, what it is more significant, the evolution of  $\alpha$  is completely independent of the rest of bioimpedance parameters. It seems that  $\alpha$  follows some sort of induced damage that has nothing to do with the cellular edema. We do believe that  $\alpha$  is closely related with the morphology of the extra-cellular spaces and this paper is intended to show evidences in this sense:

- 1) By performing computer simulations, here it is shown that the morphology of the extra-cellular spaces will indeed determine the value of  $\alpha$ .
- 2) Since the cell morphology depends on the cytoskeleton we have decided to test the effect of a drug (Swinholide A) that alters the cytoskeleton because it severs actin filaments and sequesters actin dimers [55].

It must be noted that there are some previous works that indicate that deviations from the Cole model are related somehow to cell aggregation or culsterization. For instance, it has been shown that  $\alpha$  decreases when blood hematocrit increases [56;56] or that dispersion broadening occurs during embryogenesis [57]. In this sense, the present paper can be considered a reinforcement of that interpretation.

### 5.3.2. Computer simulations

The bioimpedance simulator described in chapter 4 was employed in two cases. The idea behind those simulations was to demonstrate that, when these elements are



combined because of the complex structure of living tissues, the overall response can differ from the simple Fricke-Morse model and approach to the Cole model.

*Generic tissue (already presented in chapter 4)*

Several tries were performed with the *Bioimpedance Simulator* to produce the Cole responses by randomizing cells sizes and shapes and, the only successful results were obtained when unrealistic large differences in cell sizes were introduced. On the other hand, realistic structures such as that shown in Figure 5.9 produced Cole compatible responses with  $\alpha$  values around 0.8. ( From that kind of simulations it was concluded that the extracellular space morphology is a key factor concerning the  $\alpha$  value: the more tortuous it is, the lower  $\alpha$  value is obtained

The electrical bioimpedance of a structure resembling an generic tissue cut (Figure 5.9(a)) was obtained by the 'Bioimpedance Simulator'. It represents three cell clusters separated by large extracellular spaces (vessels). The results (Figure 5.9(b)) not only differ from the capacitive behavior (Fricke-Morse model) but also match the Cole response found in actual measurements. By using a commercial software (ZView, Scribner Associates, Inc) the following values are obtained for the Cole equation (1):  $R = 18.7 \text{ k}\Omega$ ,  $\Delta R = 127.6 \text{ k}\Omega$ ,  $\alpha = 0.835$  and  $\tau = 2.88 \text{ }\mu\text{s}$ . It must be noted that the Cole behavior disappears ( $\alpha$  tends to 1) if the extra-cellular spaces are widened.

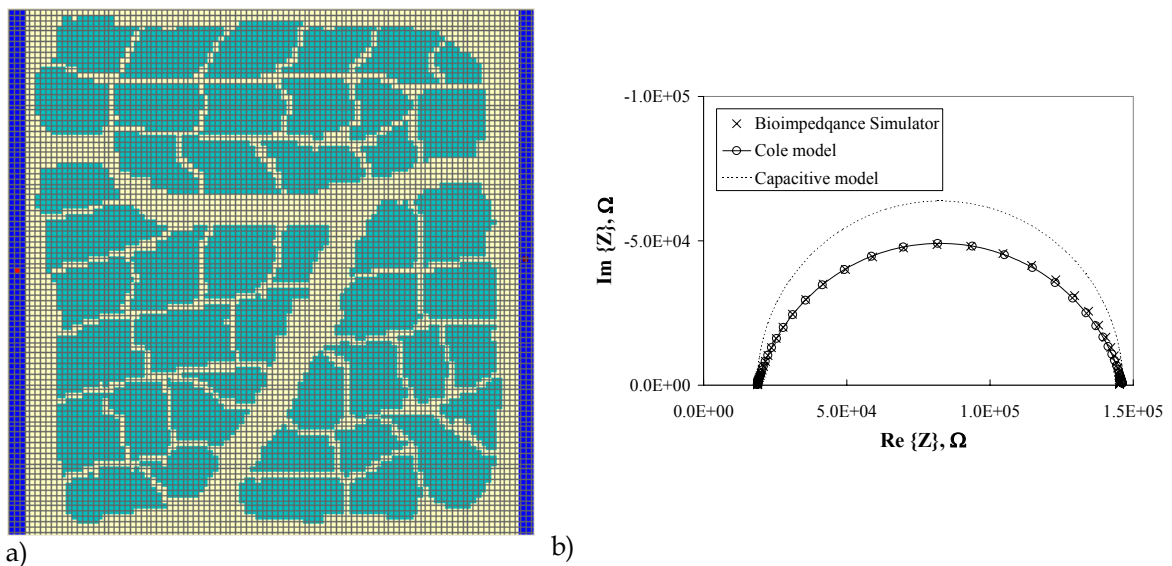


**Figure 5.9.** (a) Simulated structure resembling an actual tissue cut (100×100 squares, slice thickness=50  $\mu\text{m}$ , pixel size = 2  $\mu\text{m}$ , membrane capacitance = 1  $\mu\text{F}/\text{cm}^2$ , plasm resistivity = cytoplasm resistivity = 100  $\Omega\cdot\text{cm}$ , electrode resistivity = 0.001  $\Omega\cdot\text{cm}$ ). (b) Nyquist plot of the simulated tissue impedance.

### Kidney tissue

In order to link the simulations to the experimental study described below, a slab of kidney tissue was also modeled. Figure 5.10.a shows the simulated cross section of renal tubules. Observe that each tubule has been simulated as a single cell with a large plasma vesicle inside it. Of course, that is not realistic since each tubule is formed by multiple cells but, considering the tight packaging of these cells and the presence of inter-cellular junctions (gap junctions), it is a reasonable simplification. In Figure 5.10.c it has been represented the obtained impedance locus for this case, the response can be nicely modeled by a Cole response with  $\alpha = 0.95$ . In the case that some degree of imperfections are added to the structure (Figure 5.10.b), the impedance response significantly differs from the original one, specially for the  $\alpha$  value (from 0.95 to 0.92). The added imperfections try to mimic the detachment between the tubule cells that has been observed in Scanning Electron Microscopy (SEM) micrographs after preservation when the kidneys were treated with Swinholide A (see experimental section).

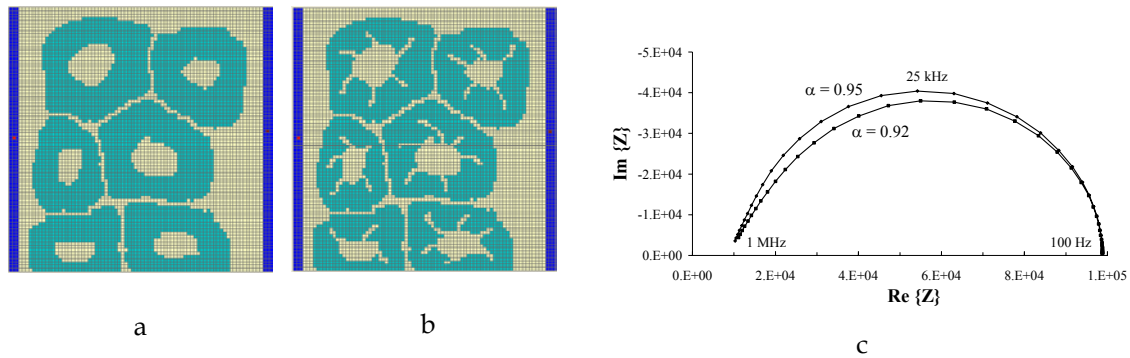


**Figure 5.10.** Simulated cross sections of renal tubules (a,b) and the obtained responses (c). (simulation parameters:  $80 \times 80$  squares, slice thickness =  $50 \mu\text{m}$ , pixel size =  $2 \mu\text{m}$ , membrane capacitance =  $1 \mu\text{F}/\text{cm}^2$ , plasma resistivity = cytoplasm resistivity =  $100 \Omega \cdot \text{cm}$ , electrode resistivity =  $0.001 \Omega \cdot \text{cm}$ ).

#### 5.3.3. Experimental study

In a previous experimental study [58], we found that the evolution of  $\alpha$  during the preservation of rat kidneys was significantly altered in the case that a warm ischemia episode was induced before kidney extirpation and preservation. Two rat kidney groups were studied during 24 hours of preservation in University of Wisconsin solution (UW): a control cold ischemia group and another group subjected previously to 45 minutes of warm ischemia. The time constant and the high frequency resistivity parameters derived from the Cole equation were able to discriminate between both groups at the beginning of the preservation ( $\Delta\tau \sim 78\%$ ,  $\Delta R_\infty \sim 36\%$ ), but these differences tended to converge as preservation time advanced. On the other hand, the  $\alpha$  showed increasing significant differences until 24h of preservation ( $\Delta\alpha \sim 15\%$ ).

One of the conclusions drawn from that study was that  $\alpha$  apparently followed the cellular morphology changes caused by cytoskeleton disruption during the preservation [59]. This fact motivated the study presented here: to add a drug that severely disrupts the cytoskeleton in order to reinforce the hypothesis that  $\alpha$  is somehow linked to the cell morphology.

Electrical bioimpedance of rat kidneys was monitored during 24 hours of preservation in three groups (4 animals per group):

- 1) Cold ischemia group (CI): kidneys were isolated and preserved for 24 hours in University of Wisconsin (UW) preservation solution.
- 2) Warm ischemia group (WI+CI): kidneys underwent a prior 45 minutes of warm ischemia before isolation and cold storage.
- 3) Swinholide group (CI+SwinA): kidneys were treated with Swinholide A (flushed 500 $\mu$ l of UW containing 500nM of SwinA) and followed the same procedure as for those in the CI group.

The study was performed using male Wistar rats weighing between 250-300 g. Animals were anesthetized by injection of sodium pentobarbital (30 mg/kg.) and placed in a supine position, keeping body temperature between 36°C and 37°C. All procedures were conducted under the supervision of our institution's Research Commission and followed EU guidelines for the handling and care of laboratory animals (see [58] for further methodological details).

Electrical bioimpedance was measured by using a miniaturized probe that consisted of four platinum electrodes (300  $\mu$ m  $\times$  300  $\mu$ m) on a needle shape silicon substrate (9mm insertion length; 600  $\mu$ m  $\times$  500  $\mu$ m cross section). An analysis of the probe properties and a description of the instrumentation system can be found elsewhere [41].

As it can be observed in figure 4, the WI+CI and the CI+SwinA groups produced a similar response for the  $\alpha$  parameter: a significant faster decrease than for the case of CI group. The other parameters ( $R_{\infty}$ ,  $R_0$  and  $\tau$ ) were different between three groups at the beginning of the preservation (see [58]) but converged after 24 hours. SEM micrographs revealed a lower degree of disruption of neighboring cell junctions in the CI group.

#### 5.3.4. Discussion

Up to now, no agreement exists on the physical meaning of the  $\alpha$  parameter in the Cole equation for the case of living tissues. Several theories have been proposed but none of them is able to completely explain all the associated phenomena. Probably all the postulated causes do certainly contribute to the  $\alpha$  value and the main point would be to identify which one represents the most significant contribution. Here it is proposed that the  $\alpha$  value is related with the morphology of the extra-cellular spaces that, of course, depends on the morphology of the cells. That is not necessarily opposite to

previous theories, it can be regarded as another interpretation. However, here this explanation is supported by strong evidences.

The dependence of the  $\alpha$  parameter on the morphology of the extra-cellular spaces can be understood intuitively. In the equivalent electrical circuit of the Cole equation (Figure 5.11) the Constant Phase Element (CPE) is depicted [35]. The behavior of this non-physical element is equivalent to a resistance-capacitance series combination whose values depend on the frequency. Such a behavior is also observed in the interface between a solid electrode and an electrolyte [60]. In this case, the CPE response has been intensively studied and it has been found that the  $\alpha$  value could depend on the morphology and the dimensions of the electrode surface irregularities [61-63]. If these irregularities are seen as pores, it can be explained intuitively the dependence of the CPE on the frequency (see Figure 5.12): as frequency increases, the electrode area 'seen' by the current from the electrolyte is reduced and the capacitance caused by the double-layer is reduced, at the same time, the current reduces its penetration into the pore and so does the resistive component. In living tissues, the cell membrane would be equivalent to the double-layer of the electrode-electrolyte interface and the narrow extracellular spaces would be equivalent to the electrolyte pores. That is, the cell membrane area 'seen' by the injected currents into the tissue sample would depend on the frequency and so does the capacitance and the resistance. Of course, that does not explain the Cole equation but helps to understand that it is possible to obtain a dependence of the resistive and capacitive components on the frequency in the case of living tissues.

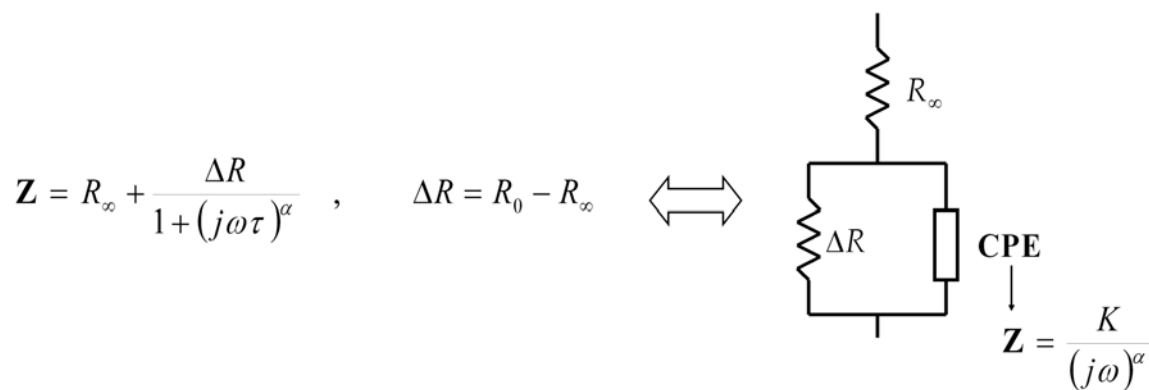


**Figure 5.11.** The Cole equation and its equivalent electrical circuit.

The computer simulations presented here show that the Cole behavior can be caused by the structure of the tissues at cell level, there is no need to assume special properties of the cell membrane or to consider the contribution of intra-cellular organelles. Moreover, other performed simulations, not shown here, including the presence of organelles or large cell dimension differences tend to produce double-dispersion responses rather than Cole responses. That is, we have found that in order to obtain impedance responses similar to the actual measurements, the key point is to consider a

more or less complex network of extra-cellular narrow spaces in which the cells are embedded.

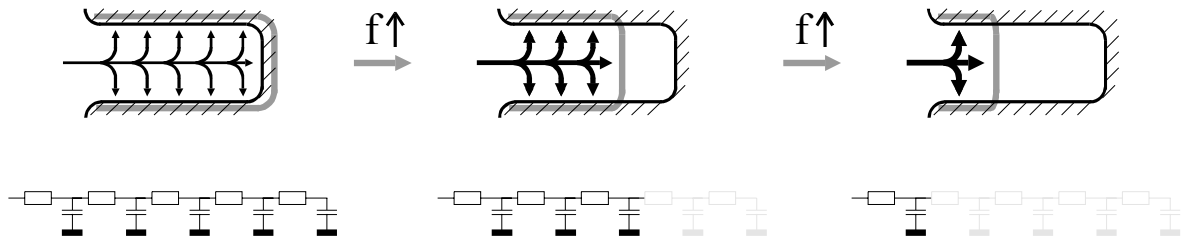


**Figure 5.12.** Representation of the electrode pore impedance dependence on frequency. As frequency increases ( $f$ ), the current tends to flow through the outer areas of the pore and that reduces the effective capacitance and the resistance .

It must be noted that the simulation of Figure 5.9 fits nicely the Cole model. In this case, some sort of fractal organization can be recognized (three clusters of cells) and that would support the fractal interpretation postulated by Dissado [53]. However, that does not imply any kind of hierarchical organization.

As it can be observed, the kidney tissue simulations do not fit so accurately the experimental measurements. The initial value of  $\alpha$  in the case of the simulation is 0.95 whereas in the experimental results is around 0.7. That is caused by the poor resolution of the simulation and an oversimplification. For instance, the presence of microvilli inside the pore is completely ignored since their diameters would be lower than the simulator resolution. However, the important fact is that the modification of the extra-cellular medium in order to mimic the cell detachment produces a decrease of the simulated  $\alpha$  value of the same order of magnitude than the actual  $\alpha$  decrease during preservation.

The experimental results reinforce the hypothesis that the  $\alpha$  parameter is related with the extra-cellular morphology. The use of Swinholide decreases the  $\alpha$  value without inducing large changes in the other Cole parameters ( $R_\infty$ ,  $R_0$  and  $\tau$ ). That implies that the  $\alpha$  parameter evolution in this case is not related with cell edema nor gap junction closure, which are common causes of bioimpedance changes. Therefore, the drug only modifies the  $\alpha$  parameter and, since this drug acts mainly on the cells cytoskeleton, it can be concluded that there exists a relation between the cytoskeleton condition and the  $\alpha$  parameter. Since there is no reason to think that the cytoskeleton by itself contributes significantly to the bioimpedance measurements, it is reasonable to think that there exists an indirect relation between it and the  $\alpha$  parameter. We do believe that this relation is caused by the direct relation between the cytoskeleton and the cell morphology.

### 5.3.5. Conclusions

It is not possible to conclude definitely that the  $\alpha$  parameter in the Cole equation is related with the extra-cellular space morphology, but, some evidences have been presented that reinforce this hypothesis.

Although the  $\alpha$  parameter is often ignored in favor of other bioimpedance parameters, here it has been demonstrated its potential application to the characterization of living tissues. Therefore, its measurement is strongly recommended since it provides independent information from other parameters such as  $R_0$  and  $\tau$ . However, it must also be mentioned that the relatively small changes of the  $\alpha$  parameter can constrain its applicability unless a fine measurement set up is employed.

## References

1. Lofgren, B., "The electrical impedance of a complex tissue and its relation to changes in volume and fluid distribution, a study on rat kidneys," *Acta Physiol.Scand.*, vol. 23, no. 81, pp. 5-50, 1951.
2. Warren, M, "Electrical Impedance of Normal and Ischemic Myocardium. Role on the Genesis of ST Segment changes and Ventricular Arrhythmias." Ph.D. Thesis Universitat Autònoma de Barcelona, 1999.
3. Noguera, N., Gómez, R., Villa, R., Ivorra, A., Aguiló, J., Pomar, J. L., and Castro, M. A. Aplicación y evaluación de un sistema para la monitorización de la preservación durante el trasplante cardiaco. 365-368. 27-11-2002. Zaragoza, Spain. XX Congreso Anual de la Sociedad Española de Ingeniería Biomédica. 27-11-2002.  
Ref Type: Conference Proceeding
4. Khabiri, E., Pomar, J. L., Ivorra, A., Gómez, R., Marimón, P., and Villa, R. Preliminary tests to assess the usefulness of an impedance microprobe for graft viability monitoring during heart preservation and transplantation. 6-10-2001. Lisboa, Portugal. 10th Congress ESOT 2001. 6-10-2001.  
Ref Type: Conference Proceeding
5. Villa, R., Mouroux, A., and Gómez, C., "A novel system for monitoring organs for transplant," *Medical Device Technology*, vol. 15, no. 3, pp. 27-29, 2004.
6. Kun, S., Ristic, B., Peura, R. A., and Dunn, R. M., "Algorithm for tissue ischemia estimation based on electrical impedance spectroscopy," *IEEE Transactions on Biomedical Engineering*, vol. 50, no. 12, pp. 1352-1359, 2003.
7. Ishida, T., Yarimizu, K., Gute, D. C., and Korthuis, R. J., "Mechanisms of ischemic preconditioning," *Shock*, vol. 8, no. 2, pp. 86-94, 1997.
8. Fiddian-Green, R. G., "Gastric intramucosal pH, tissue oxygenation and acid-base balance," *Br J Anaesth*, vol. 74, no. 5, pp. 591-606, 1995.
9. Dmochowski, J. R. and Couch, N. P., "Electrometric surface pH of the ischemic kidney and the effect of hypothermia," *J Surg Res*, vol. 6, no. 1, pp. 45-48, 1966.
10. Tonnessen, T. I. and Kvarstein, G., "PCO<sub>2</sub> electrodes at the surface of the kidney detect ischaemia," *Acta Anaesthesiol Scand*, vol. 40, no. 5, pp. 510-519, 1996.
11. Reeves, W. B. and Shah, S. V., "Activation of potassium channels contributes to hypoxic injury in proximal tubules," *J Clin Invest*, vol. 94, no. 6, pp. 2289-2294, 1994.
12. Gersing, E., "Impedance spectroscopy on living tissue for determination of the state of organs," *Bioelectrochemistry and Bioenergetics*, vol. 45 pp. 145-149, 1998.
13. Jamart, J. and Lambotte, L., "Differential effect of swelling and anoxia on kidney function and its consequences on the mechanism of action of intracellular preservation solutions," *Transplantation*, vol. 34, no. 4, pp. 176-182, 1982.
14. Lambotte, L. and Wojcik, S., "Measurement of cellular edema in anoxia and its prevention by hyperosmolar solutions," *Surgery*, vol. 83, no. 1, pp. 94-103, 1978.
15. Ueda, N., Kaushal, G. P., and Shah, S. V., "Apoptotic mechanisms in acute renal failure," *Am J Med*, vol. 108, no. 5, pp. 403-415, 2000.

16. Cochrane, J., Williams, B. T., Banerjee, A., Harken, A. H., Burke, T. J., Cairns, C. B., and Shapiro, J. I., "Ischemic preconditioning attenuates functional, metabolic, and morphologic injury from ischemic acute renal failure in the rat," *Ren Fail*, vol. 21, no. 2, pp. 135-145, 1999.
17. Riera, M., Herrero, I., Torras, J., Cruzado, J. M., Fatjo, M., Lloberas, N., Alsina, J., and Grinyo, J. M., "Ischemic preconditioning improves postischemic acute renal failure," *Transplant Proc*, vol. 31, no. 6, pp. 2346-2347, 1999.
18. Cinca, J., Warren, M., Carreño, A., Tresàncez, M., Armadans, L., Gómez, P., and Soler-Soler, J., "Changes in Myocardial Electrical Impedance Induced by Coronary Artery Occlusion in Pigs With and Without Preconditioning, Correlation With Local ST-Segment Potential and Ventricular Arrhythmias," *Circulation*, vol. 96, no. 9, pp. 3079-3086, 1997.
19. Tan, H. L., Mazon, P., Verberne, H. J., Sleswijk, M. E., Coronel, R., Ophhof, T., and Janse, M. J., "Ischaemic preconditioning delays ischaemia induced cellular electrical uncoupling in rabbit myocardium by activation of ATP sensitive potassium channels," *Cardiovascular Research*, vol. 27, no. 4, pp. 644-651, 1993.
20. Cosofret, V. V., Erdösy, M., Johnson, T. A., Buck, R. P., Ash, R. B., and Neuman, M. R., "Microfabricated sensor arrays sensitive to pH and K<sup>+</sup> for ionic distribution measurements in the beating heart," *Anal.Chem.*, vol. 67, no. 10, pp. 1647-1653, 1995.
21. Osypka, M. and Gersing, E., "Tissue impedance spectra and the appropriate frequencies for EIT," *Physiol Meas.*, vol. 16, no. 3 Suppl A, pp. A49-A55, Aug.1995.
22. Leaf, A., "Regulation of intracellular fluid volume and disease," *Am J Med*, vol. 49 pp. 291-295, 1970.
23. Molitoris, B. B., Chan, L. K., Shapiro, J. I., Conger, J., and Falk, S. A., "Loss of epithelial polarity: a novel hypothesis for reduced proximal tubule Na<sup>+</sup> transport following ischemic injury," *J Membr Biol*, vol. 107, no. 2, pp. 119-127, 1989.
24. Quast, U., "ATP-sensitive K<sup>+</sup> channels in the kidney," *Naunyn Schmiedebergs Arch Pharmacol*, vol. 354, no. 3, pp. 213-225, 1996.
25. Flores, J., DiBona, D. R., Beck, C. H., and Leaf, A., "The role of cell swelling in ischemic renal damage and the protective effect of hypertonic solute," *J Clin Invest*, vol. 51, no. 1, pp. 118-126, 1972.
26. Ogawa, T., Nussler, A. K., Tuzuner, E., Neuhaus, P., Kaminishi, M., Mimura, Y., and Beger, H. G., "Contribution of nitric oxide to the protective effects of ischemia preconditioning in ischemia-reperfused rat kidneys," *J Lab Clin Med*, vol. 138, no. 1, pp. 50-58, 2001.
27. Asimakis, G. K., Inners-McBride, K., Medellin, G., and Conti, V. R., "Ischemic preconditioning attenuates acidosis and postischemic dysfunction in isolated rat heart," *Am J Physiol*, vol. 263 pp. H997-H894, 1992.
28. Shanley, P., Shapiro, J. I., Chan, L., Burke, T. J., and Johnson, G. C., "Acidosis and hypoxic medullary injury in the isolated perfused kidney," *Kidney Int*, vol. 34, no. 6, pp. 791-796, 1988.
29. Cleveland, J. C. J., Meldrum, D. R., Rowland, R. T., Banerjee, A., and Harken, A. H., "Adenosine preconditioning of human myocardium is dependent upon the ATP-sensitive K<sup>+</sup> channel," *J Moll Cell Cardiol*, vol. 29, no. 1, pp. 175-182, 1997.



30. Cohen, M. V., Baines, C. P., and Downey, J. M., "Ischemic preconditioning. from adenosine receptor of KATP channel," *Annu Rev Physiol*, vol. 62 pp. 79-109, 2000.
31. Sola, A., Rosello-Catafau, J., Alfaro, V., Pesquero, J., Palacios, L., Gelpi, E., and Hotter, G., "Modification of glyceraldehyde-3-phosphate dehydrogenase in response to nitric oxide in intestinal preconditioning," *Transplantation*, vol. 67, no. 11, pp. 1446-1452, 1999.
32. Daemen, J. W., Oomen, A. P., Kelders, W. P., and Kootstra, G., "The potential pool of non-heart-beating kidney donors," *Clin Transplant*, vol. 11, no. 2, pp. 149-154, 1997.
33. Kievit, J. K., Oomen, A. P. A., Vries, B. d., Heineman, E., and Kootstra, G., "Update on results of non-heart-beating donor kidney transplantation," *Transplant Proc*, vol. 29 pp. 2989-2991, 1997.
34. Stubenitsky, B. M., Booster, M. H., Nederstigt, A. P., Kievit, J. K., Jacobs, R. W., and Kootstra, G., "Kidney preservation in the next millenium," *Transpl Int*, vol. 12, no. 2, pp. 83-91, 1999.
35. Grimnes, S. and Martinsen, Ø. G., *Bioimpedance and bioelectricity basics* London: Academic Press, 2000.
36. Hauet, T., Goujon, J. M., Vadewalle, A., Baumert, H., Lacoste, L., Tillement, J. P., Eugene, M., and Carretier, M., "Trimetazidine reduces renal dysfunction by limiting the cold ischemia/reperfusion injury in autotransplanted pig kidneys," *J Am Soc Nephrol*, vol. 11, no. 1, pp. 138-148, 2000.
37. Ashworth, S. L., Sandoval, R. M., Hosford, M., Bamburg, J. R., and Molitoris, B. A., "Ischemic injury induces ADF relocalization to the apical domain of rat proximal tubule cells," *Am J Physiol Renal Physiol*, vol. 280, no. 5, pp. F886-F894, 2001.
38. Herrero, I., Torras, J., Carrera, M., Castells, A., Pasto, L., Gil-Vernet, S., Alsina, J., and Grinyo, J. M., "Evaluation of a preservation solution containing fructose-1,6-diphosphate and mannitol using the isolated perfused rat kidney. Comparison with Euro-Collins and University of Wisconsin solutions," *Nephrol Dial Transplant*, vol. 10, no. 4, pp. 519-526, 1995.
39. Genescà, M., Sola, A., Miquel, R., Pi, F., Xaus, C., Alfaro, V., and Hotter, G., "Role of changes in tissular nucleotides on the development of apoptosis during ischemia/reperfusion in rat small bowel," *Am J Pathol*, vol. 161, no. 4, pp. 1839-1847, 2002.
40. Goujon, J. M., Hauet, T., Menet, E., Levillain, P., Babin, P., and Carretier, M., "Histological evaluation of proximal tubule cell injury in isolated perfused pig kidneys exposed to cold ischemia," *J Surg Res*, vol. 82, no. 2, pp. 228-233, 1999.
41. Ivorra, A., Gómez, R., Noguera, N., Villa, R., Sola, A., Palacios, L., Hotter, G., and Aguiló, J., "Minimally invasive silicon probe for electrical impedance measurements in small animals," *Biosensors & Bioelectronics*, vol. 19, no. 4, pp. 391-399, 2003.
42. Sperelakis, N. and Sfyris, G., "Impedance Analysis Applicable to Cardiac Muscle and Smooth Muscle Bundles," *IEEE Transactions on Biomedical Engineering*, vol. 38, no. 10, pp. 1010-1022, 1991.
43. Haemmerich, D., Ozkan, O. R., Tsai, J. Z., Staelin, S. T., Tungjitkusolmun, S., Mahvi, D. M., and Webster, J. G., "Changes in electrical resistivity of swine liver after occlusion and postmortem," *Med.Biol.Eng.Comput.*, vol. 40 pp. 29-33, 2002.

44. Konishi, Y., Morimoto, T., Kinouchi, Y., Iritani, T., and Monden, Y., "Electrical properties of extracted rat liver tissue," *Research in Experimental Medicine*, vol. 195 pp. 183-192, 1995.
45. Genescà, M., Ivorra, A., Sola, A., Palacios, L., Goujon, J. M., Hauet, T., Villa, R., Aguiló, J., and Hotter, G., "Electrical bioimpedance measurement during hypothermic rat kidney preservation for assessing ischemic injury," *Biosensors & Bioelectronics*, vol. Accepted for publication 2004.
46. Keese, C. R. and Giaever, I., "A Biosensor that Monitors Cell Morphology with Electrical Fields," *IEEE Engineering in Medicine and Biology Magazine*, vol. 13, no. 3, pp. 402-408, 1994.
47. Cole, K. S., *Membranes, Ions and Impulses* Berkeley: University of California Press, Ltd., 1972.
48. Schwan, H. P., "Electrical properties of tissue and cell suspensions," in Lawrence, J. H. and Tobias, C. A. (eds.) *Advances in Biological and Medical Physics* New York: Academic Press, 1957.
49. Cole, K. S. Permiability and impermiability of cell membranes for ions. 8, 110-122. 1940. Cold Spring. Sympos Quant Biol.  
Ref Type: Conference Proceeding
50. Foster, K. R. and Schwan, H. P., "Dielectric properties of tissues and biological materials: a critical review," *CRC Critical Reviews in Biomedical Engineering*, vol. 17 pp. 25-104, 1989.
51. Ackmann, J. J. and Seitz, M. A., "Methods of complex impedance measurements in biologic tissue," *Critical Reviews in Biomedical Engineering*, vol. 11 pp. 281-311, 1984.
52. Raicu, V., Saibara, T., Enzan, H., and Irimajiri, A., "Dielectric properties of rat liver in vivo: analysis by modeling hepatocytes in the tissue architecture," *Bioelectrochemistry and Bioenergetics*, vol. 47 pp. 333-342, 1998.
53. Dissado, L. A., "A fractal interpretation of the dielectric response of animal tissues," *Phys.Med.Biol.*, vol. 35, no. 11, pp. 1487-1503, 1990.
54. Raicu, V., Saibara, T., and Irimajiri, A., "Multifrequency method for dielectric monitoring of cold-preserved organs," *Phys.Med.Biol.*, vol. 45 pp. 1397-1407, 2000.
55. Bubb, M. R. and Spector, I., "Use of the F-actin-binding drugs, misakinolide A and swinholide A," *Methods Enzymol*, vol. 298 pp. 26-32, 1998.
56. Fomekong, R. D., Pliquett, U., and Pliquett, F., "Passive electrical properties of RBC suspensions: changes due to distribution of relaxation times in dependence on the cell volume fraction and medium conductivity," *Bioelectrochemistry and Bioenergetics*, vol. 47 pp. 81-88, 1998.
57. Asami, K. and Irimajiri, A., "Dielectrospectroscopic monitoring of early embryogenesis in single frog embryos," *Phys.Med.Biol.*, vol. 45 pp. 3285-3297, 2000.
58. Genescà, M., Ivorra, A., Sola, A., Palacios, L., Villa, R., and Hotter, G. Electrical bioimpedance monitoring of rat kidneys during cold preservation by employing a silicon probe. 127-130. 2004. Gdansk, Poland. Proceedings from the XII International Conference on Electrical Bio-Impedance (ICEBI). 20-6-0004.  
Ref Type: Conference Proceeding

59. Breton, S. and Brown, D., "Cold-induced microtubule disruption and relocalization of membrane proteins in kidney epithelial cells," *J Am Soc Nephrol*, vol. 280, no. 4, pp. 619-627, 1998.
60. McAdams, E. T., "Effect of surface topography on the electrode-electrolyte interface impedance, 1. The High Frequency ( $f > 1$  Hz), Small Signal, Interface Impedance - A Review," *Surface Topography*, vol. 2 pp. 107-122, 1989.
61. De Levie, R., "The influence of surface roughness of solid electrodes on electrochemical measurements," *Electrochimica Acta*, vol. 10 pp. 113-130, 1965.
62. Nyikos, L. and Pajkossy, T., "Fractal dimension and fractional power frequency-dependent impedance of blocking electrodes," *Electrochimica Acta*, vol. 30, no. 11, pp. 1533-1540, 1985.
63. Liu, S. H., "Fractal Model for the ac Response of a Rough Interface," *Physical Review Letters*, vol. 55, no. 5, pp. 529-532, July 1985.

